Chapter

Imaging of Tendons

Stephanie C. Torres-Ayala, Alvaro Bravo-Martínez, Amanda P. Marrero-González, Luis R. Rodriguez-Ortíz and Jorge A. Vidal

Abstract

Magnetic resonance imaging (MRI) and ultrasound (US) are useful radiologic modalities that allow adequate evaluation of tendon anatomy and integrity. Each modality contains unique advantages as diagnostic tools, allowing detection of tendon injuries and pathology. This chapter focuses on the key imaging features of tendons in both ultrasound and magnetic resonance, with emphasis on the major joints such as the shoulder, elbow, hand/wrist, hip, knee and foot/ankle joints. Each section provides a review of standard magnetic resonance imaging protocols and ultrasound technique, along with a discussion of the radiologic appearance of the most common tendon pathology affecting each joint.

Keywords: tendons, ultrasound, magnetic resonance imaging, radiology

1. Introduction

Imaging modalities play a significant role in the evaluation of tendon pathology. Knowledge of anatomical landmarks of the tendons is of utmost importance in order to differentiate and accurately diagnose pathologic processes. Ultrasound (US) and Magnetic Resonance Imaging (MRI) are currently the imaging modalities of choice to evaluate tendon pathology, each with its own unique advantages as diagnostic tools. Tendons are characteristically seen as echogenic fibrillar structures on US and as homogeneous hypointense structures on MRI.

This chapter focuses on the key imaging features of tendons in US and MRI modalities, with emphasis on the shoulder, elbow, hand, hip, knee and foot joints. Each chapter section will provide a review of the anatomical landmarks, normal US and MRI appearance, imaging protocols, and discussion of common pathology affecting the tendons in each joint.

2. Shoulder

2.1 MRI protocol

The patient is positioned supine with the arm at the side in neutral position or slight external rotation in order to put some tension on the long head of the biceps tendon. A small field of view (approximately 14–16 cm) is obtained in three imaging planes: axial, coronal oblique, and sagittal oblique. The axial images are acquired from the top of the acromioclavicular joint through the proximal humeral shaft including the insertion of the pectoralis muscle. The coronal oblique images are obtained with planes made parallel to the supraspinatus tendon or in a plane perpendicular to the articular surface of the glenoid, ranging from the coracoid process to the infraspinatus muscle. Finally, the sagittal oblique images are acquired with planes parallel to the articular surface of the glenoid, from the scapular neck through the lateral aspect of the humerus [1]. A standard shoulder MRI usually includes sagittal oblique T1-weighted image (T1WI), fast spin echo (FSE) T2-weighted image (T2WI) with fat suppression, coronal oblique FSE T2WI with fat suppression, and axial FSE T2WI and FSE proton density (PD) with fat suppression.

2.2 Ultrasound examination technique

Sonographic evaluation of the shoulder can be performed with the following steps [2]:

1. Long head of biceps brachii tendon: The patient places the hand on his or her lap, as this position rotates the bicipital groove anteriorly. The transducer is placed in the axial plane over the anterior aspect of the shoulder to identify the bicipital groove, where the long head of the biceps brachii tendon is found. The long head of the biceps brachii tendon is followed proximally to where the bicipital groove becomes shallow and then distal to the level of the pectoralis major tendon. The transducer is then turned 90° to visualize the tendon in long axis from the humeral head to the pectoralis tendon.

2. Subscapularis tendon: The transducer is placed in the axial plane, as in the previous step, to first visualize the bicipital groove and then centered over the lesser tuberosity at the medial aspect of the bicipital groove. Then the patient rotates the shoulder externally to pull the subscapularis tendon laterally, which will orient the tendon fibers perpendicular to the transducer sound beam and eliminate anisotropy. Then it may be moved laterally over the bicipital groove to ensure that the long head of the biceps brachii tendon is within the bicipital groove, and rule out subluxation or dislocation, which may be present only in external rotation [3]. The subscapularis tendon can also be evaluated in short axis by turning the transducer 90°.

3. Supraspinatus and infraspinatus tendon: One way to evaluate the supraspinatus tendon is to ask the patient to place the dorsum of his or her ipsilateral hand behind the back, called the Crass position [4]. This position pulls the tendon out from under the acromion. The Crass position is very helpful in localizing the greater tuberosity but its limitations include poor visualization of the rotator interval and patient discomfort [3]. Because of these disadvantages the modified Crass position is more commonly used, by asking the patient to place his or her ipsilateral hand on the hip or buttock region. This position places the greater tuberosity more lateral than with the Crass position, and also allows easy visualization of the rotator interval with little patient discomfort [5]. Either in the Crass or modified Crass position, supraspinatus evaluation should begin by observing the tendon in long axis as this allows visualization of the three surfaces (articular, bursal, greater tuberosity) [6]. Scanning should be continued anteriorly along the greater tuberosity until the intra-articular portion of the biceps tendon is identified. The infraspinatus tendon is evaluated by moving the transducer posteriorly over the middle facet of the greater tuberosity.

2.3 Supraspinatus tendon

The supraspinatus tendon arises from the supraspinous fossa, runs between the undersurface of the acromion and the top of the humeral head, and inserts into the most superior facet of the greater tuberosity of the humerus. On MRI, the entire length of the supraspinatus tendon can be seen well in the coronal oblique plain, running at an angle of approximately 45° [7]. The musculotendinous junction of the tendon normally is located just lateral to the acromioclavicular joint. On sagittal oblique images, the supraspinatus tendon is imaged in cross section, which is valuable to confirm the status of the tendon when abnormalities are seen in the plane of imaging, where the tendon is viewed longitudinally.

The normal sonographic appearance of the supraspinatus tendon is hyperechoic and fibrillar with a convex superior margin at the level of the superior facet of the greater tuberosity of the humerus [8]. It parallels the curved contour of the humeral head, flattening out as it inserts into the greater tuberosity. The subacromial-subdeltoid bursa should be seen as a single thin hyperechoic line paralleling the tendon superiorly.

The supraspinatus tendon is the most commonly affected when compared to the other tendons of the shoulder [8]. There are multiple pathologies that may limit the space within the coracoacromial arch, producing impingement of this tendon. Abnormalities from impingement range from tendon degeneration to partial-thickness or full-thickness tears. Most partial-thickness tears occur in the articular aspect of the tendon, rather than on the bursal surface. Tears are usually located distally, either near its attachment to the greater tuberosity or in the critical zone located approximately 1 cm proximal to its insertion, and start in the anterior portion as rim rent tears and spread posteriorly [7]. Rim rent tears refer to disruption of the insertional fibers on the greater tuberosity. Complete disruption of the fibers with communication between the joint and the overlying bursa indicates a full-thickness tear (**Figure 1**).

Tendon degeneration usually demonstrates increased signal intensity on T1WI and T2WI, although not as high signal as fluid. However, a partial thickness tear demonstrates increased signal intensity on T2WI similar to fluid. Indications of a full thickness tear include: tendon discontinuity, fluid signal in tendon gap, and retraction of musculotendinous junction [7].

Tears in ultrasound are demonstrated as anechoic or hypoechoic defects, although acute tears will more likely appear anechoic like fluid [8]. As a supraspinatus tendon tear enlarges, tendon retraction and volume loss occur, with loss of the normal superior convex shape. The length or degree of retraction of a full thickness tear can be measured on longitudinal views oriented parallel to the long axis of the cuff and the width can be measured on transverse views oriented perpendicular to the long axis of the cuff [2]. On the other hand, tendinosis is usually less defined, and may be associated with increased tendon thickness, and not usually associated with adjacent cortical irregularity of the greater tuberosity.

2.4 Long head of biceps brachii tendon

The long head of biceps brachii tendon originates from the supraglenoid tubercle of the scapula, courses intra-articularly to the entrance of the bicipital groove and continues caudally, inserting along the radial tuberosity of the proximal radius. On MRI, portions of this tendon can be evaluated on coronal oblique images, from its origin at the superior labrum and inferiorly in the bicipital groove. The portion that is located within the bicipital groove is seen on axial images as a round or oval structure, and sometimes it may blend with the low signal intensity cortex of the humerus, making it difficult to identify. It is normal to find a small amount of fluid

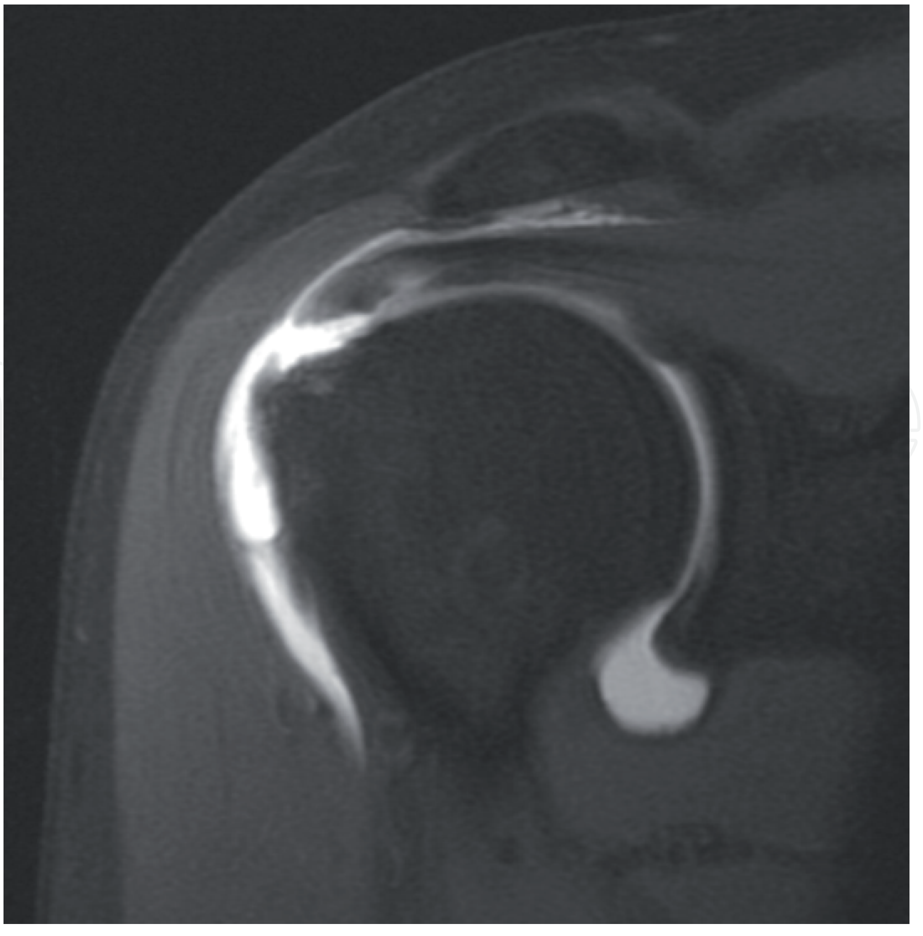

Figure 1.
Magnetic resonance arthrogram T1 fat saturated coronal oblique image shows a full thickness tear of the supraspinatus tendon with contrast leaking from the joint capsule into the subdeltoid space.

in the dependent side of the long head of the biceps tendon sheath, as the tendon sheath normally communicates with the glenohumeral joint. High signal round structures found lateral to the tendon within the bicipital groove represent the anterior circumflex humeral artery/vein and should not be confused with tenosynovitis [7].

The long head of biceps brachii tendon should be found within the intertubercular groove upon sonographic evaluation of the shoulder. The tendon fibers should be seen without tears, heterogeneity or thickening. The normal tendon will appear hyperechoic; however, because the tendon courses deep, it may appear artifactually hypoechoic due to anisotropy [8]. Adjusting the transducer to aim the sound beam perpendicular to the tendon fibers can eliminate this artifact.

The proximal aspect of the tendon may be affected by impingement in the same ways as the supraspinatus tendon because of its similar location and course beneath the supraspinatus tendon. Tears associated with impingement usually occur proximal to the bicipital groove and are usually seen in the older population. Acute tears unrelated to impingement are commonly secondary to a traumatic injury in young individuals, and usually occur distally in the tendon, near the musculotendinous junction [7]. When a full-thickness tear occurs, axial MRI images of the shoulder may show an empty bicipital groove, without evidence of the oval, low signal long head of the biceps tendon. An empty bicipital groove may also indicate tendon dislocation, which is also associated with disruption of the transverse humeral ligament that holds the biceps tendon in place. In this case, the low signal round tendon is seen medial to the bicipital groove, either deep or superficial to the subscapularis tendon, which usually also tears as well.

When shoulder effusion is present, fluid may be seen sonographically surrounding the biceps tendon at the level of the bicipital groove given the normal communication between the tendon sheath and joint. Joint effusion appears anechoic, however if fluid is complex it may be hypoechoic, isoechoic or hyperechoic relative to muscle, resembling synovial hypertrophy [8]. Tenosynovitis is favored over joint fluid extending into the sheath if there is focal distention of the tendon sheath with hyperemia and it is symptomatic with transducer pressure. Tendinosis of the long head of the biceps brachii should be considered when the tendon is abnormally hypoechoic and increased in thickness with lack of fiber disruption. Anechoic clefts or surface irregularity of the tendon favor a partial-thickness tear [9]. The primary finding in a full-thickness tear is lack of visualization of the biceps tendon or empty bicipital groove. As mentioned before, one must also consider tendon subluxation or dislocation when encountered with an empty bicipital groove. In this case, the tendon can be seen medially displaced, usually superficial to the lesser tuberosity.

3. Elbow

3.1 MRI protocol

Patients should be supine in a comfortable position with the arm to be imaged in supine position as well. Images should include from the distal humeral metaphysis up to the radial tuberosity and this area should be imaged in axial, coronal and sagittal planes. Sequences should include non-fat saturated T1, PD, and fat-saturated T2WI; gradient echo (GRE) may also be included depending on the pathology suspected [10].

3.2 Ultrasound examination technique

Ultrasound of the elbow usually focuses on the area of clinical interest, nonetheless, the anterior, lateral, medial and posterior compartments should all be evaluated. A high frequency linear transducer of 12–17 mHZ is preferred. To evaluate the anterior compartment of the elbow, which includes the distal biceps tendon, it should be extended with a supine forearm. Evaluation should include transverse and longitudinal planes from 5 cm proximal and distal to the joint. The lateral elbow compartment, which includes the common extensor tendon, is evaluated with the arm placed in internal rotation and elbow joint in flexion. The medial compartment includes the common flexor tendons, which is evaluated sonographically by extending the forearm in forceful external rotation. Lastly, the posterior elbow, which contains the distal triceps tendon, is evaluated by placing the elbow in 90° flexion with the arm internally rotated [11].

3.3 Common extensor tendon

The common extensor tendon attaches to the humeral lateral epicondyle uniting the individual tendons of the extensor carpi radialis brevis, extensor digitorum, extensor digiti minimi and the extensor carpi ulnaris. Normally the common extensor tendon is a band of low signal intensity on both T1WI and T2WI, seen superficial to the radial collateral ligament complex and the tendon should show complete fibers at its insertion in the lateral epicondyle.

A common cause for elbow pain is lateral epicondylitis, also known as tennis elbow. In these cases, the tendon may appear thickened with increased intermediate signal intensity on T1WI and T2WI. Abnormal fluid signal intensity may be seen traversing the tendon fibers in partial tendon tears, most common in the extensor carpi radialis brevis tendon [12] (**Figure 2**). If there is a fluid signal intensity gap with discontinuity of the tendon fibers, a full thickness tear is present. Avulsion injuries may be present when there is associated bone marrow edema at the tendinous insertion site. The US evaluation of lateral epicondylitis shows a heterogeneous tendon with focal hypoechoic areas.

3.4 Distal biceps tendon

The distal biceps brachii tendon is located at the anterior elbow compartment, coursing through the antecubital fossa with its distal insertion at the radial bicipital tuberosity. Its superficial fibers form the lacertus fibrosis which course medially to form the distal portion of the tendon. Pathology of the distal biceps tendons is most common in people who perform heavy weightlifting, with increased risk in those who use anabolic steroids [12]. A distal biceps tendon tear results in retraction of the myotendinous junction, clinically known as a Popeye's sign or mass in the proximal arm. This is seen as complete discontinuity of the tendon fibers, best appreciated in axial and sagittal planes. In order to be able

Figure 2.
Proton density fat saturated coronal image of the elbow shows fluid signal at the insertion of the common extensor tendon consistent with a tendon tear.

to visualize the retracted tendon and area of avulsion at its distal insertion the arm may be supine, flexed and abducted. If there is a partial tear present, then on magnetic resonance imaging there will be peritendinous increased T2 signal intensity [12].

4. Hand/wrist

4.1 MRI protocol

For MR imaging of the hand the patient is placed in prone position, with the arm elevated above the head, also known as the "superman position". When specifically imaging the thumb, the latter should be fully extended and at the center of the scanner and foam pads may be used for fixation of the area of interest. Small surface or dedicated hand or wrist coils are important in order to obtain high quality images. Axial images with respect to the fingers are first obtained and these are then used to plan sagittal and coronal views. When imaging the thumbs, coronal and sagittal views should be tilted 90° to sesamoids at the level of the metacarpophalangeal joint (**Figure 3**) [13]. It is always important to include adjacent fingers within the field of view of the image for comparison [14]. Three-Tesla MRIs are preferred due to the high resolution and detail provided for these small anatomical regions. Standard sequences used to evaluate for hand tendinous or ligamentous injury are: coronal PD, axial T1, coronal T1, sagittal T1, axial T2 and sagittal T2W sequences. When evaluating the wrist, the wrist should be at the center of the scanner with dedicated surface coils as well. Coronal images should be oriented between the radial and styloid ulnar processes and sagittal images prescribed 90° to coronals. The axial images should include approximately 2–3 cm proximal to the radiocarpal joint and at least 1 cm distal to the carpometacarpal joints [13].

4.2 Ultrasound examination technique

US of the wrist and hand are usually tailored to an area of interest, according to patient symptoms. The wrist is separated into a dorsal and ventral compartment. The hand is placed in prone position and a transverse sweep allows evaluation of the 6-extensor compartments. The hand is later supinated, allowing evaluation of the carpal tunnel and Guyon's canal.

4.3 De Quervain tenosynovitis

It is the second most common stenosing synovitis, presenting with pain and swelling at the styloid process region when moving the thumb or wrist. Anatomically, the abductor pollicis longus (APL) and extensor pollicis brevis (EPB) tendons are held within a fibro-osseous sheath called the extensor retinaculum. Repetitive trauma results in thickening of the tendons and retinaculum resulting in inflammation and edema. In some cases, a septum has been found between both tendons, thought to worsen symptoms.

On US, the APL and EPB tendons are thickened at the level of the radial styloid with increased fluid within the first extensor compartment. A halo sign has been described, secondary to peritendinous subcutaneous edema. Doppler imaging should show increased vascularity secondary to hyperemia and inflammation [15].

Figure 3.
On the left side, we have a T2WI showing the tendon as a hypointense structure; while on the right side we see a composite US image of the flexor tendon of the finger with some areas of anisotropy.

On MRI, tenosynovitis is seen as increased signal intensity on T2WI and low to intermediate signal on T1WI of the tendon sheath. The retinaculum will also appear thickened with increased T2 signal intensity. When the tendon is thickened, mostly seen at the radial styloid at its medial aspect, with increased T1 and T2 intra-tendinous signal and a striated tendinous signal, tendinosis is said to be present. These may also be accompanied by a longitudinal tendinous tear, where linear T2 signal will be seen traversing the tendon, most common in the APL, due to fluid within the tendinous rupture.

4.4 Flexor tendon/trigger finger

Trigger finger is a stenosing tenosynovitis secondary to repetitive microtrauma. This results in inflammation and thickening of the flexor tendon and tendon sheath, causing transient locking of the digit in a flexed position.

DOI: http://dx.doi.org/10.5772/intechopen.84521

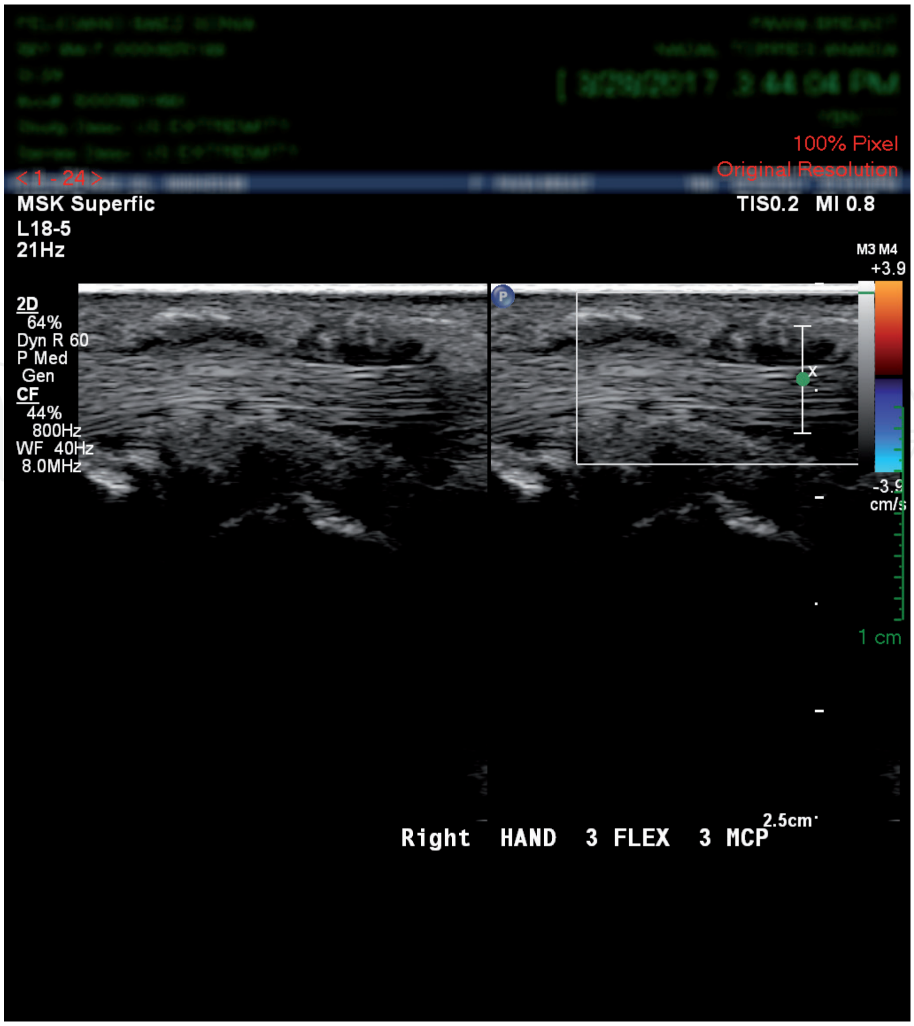

Figure 4.
Thickening of the A1 pulley in the 3rd flexor tendon of the hand consistent with clinical picture of "trigger finger".

This pathology is mainly evaluated with US instead of MRI (**Figure 4**). On US, the flexor tendon and A1 pulley will be thickened with a diameter greater than 1.1 mm. Hypoechoic fluid may also be seen around the tendon sheath, representing an effusion [16].

5. Knee

5.1 MRI protocol

The knee is positioned in a relaxed state, with about 5° of external rotation so that the anterior cruciate ligament is orthogonal to the sagittal plane of imaging. A small field of view is used, usually between 14 and 16 cm, and multiplanar imaging is obtained with coronal, sagittal, and axial images [17]. Sequences of a knee MRI should include any combination of fluid-sensitive sequences with anatomic sequences. Fluid-sensitive images can be either fat-sat PDW, or T2W spin-echo images versus STIR images. Anatomic sequences may include either T1W or PDW, spin-echo images [18].

5.2 Ultrasound examination technique

Ultrasound evaluation may be completed with the patient supine, although the posterior structures are better seen in the prone position [19]. Examination may be focused over the area that is relevant to the patient's history; nonetheless a complete examination of all areas should be performed. Sonographic examination may be divided in four methods: anterior, medial, lateral, and posterior evaluation of the knee.

1. Anterior knee: Evaluated with patient in a supine position and knee slightly flexed 20–30°. The primary structures evaluated in this approach include the quadriceps tendon, patella, patellar tendon, patellar retinaculum, suprapatellar joint recess, the medial and lateral recesses, and the anterior knee bursae [20]. Evaluation begins with transducer in the sagittal plane, proximal to the patella, to evaluate the quadriceps tendon. Deep to the quadriceps tendon, the suprapatellar recess is identified. Next, the transducer is moved inferiorly in the sagittal plane to evaluate the patellar tendon. The transducer is then moved to both the medial and lateral margins of the patella in the transverse plane, to evaluate the medial and lateral patellar retinacula, and the underlying medial and lateral recesses. Finally, the knee is placed in a 90° flexed position to evaluate the femoral trochlear cartilage in the transverse plane superior to the patella.

2. Medial knee tendons: The patient remains supine and rotates hip externally for evaluation of the medial aspect of the knee. The tendinous structures that are evaluated in this region are the pes anserine tendons [19].

3. Lateral knee: The patient is in supine position, with internal rotation of the hip, and knee slightly flexed. The key structures that are examined include the iliotibial band, lateral collateral ligament (LCL), biceps femoris tendon, popliteus, common peroneal nerve, and body and anterior horn of the lateral meniscus [19]. The transducer may be initially placed over the long axis of the patellar tendon, and then moved laterally to identify the iliotibial band. Next, the transducer is moved laterally to the coronal plane over the lateral femoral condyle to identify the groove for the popliteal tendon, an important bone landmark. Using this groove as a landmark, the proximal end of the transducer is stabilized on the femur, and the distal aspect is rotated posterior to visualize the fibular head. At this site, LCL is identified. After the transducer is moved along the LCL to its fibular attachment, the distal end of the transducer is anchored to the fibular head while the proximal aspect is rotated posteriorly in the coronal plane to visualize the biceps femoris tendon. As the transducer is moved posteriorly from the coronal plane view, the common peroneal nerve can be identified. Upon return to the popliteal groove, the distal popliteal tendon may be followed.

4. Posterior knee: The posterior aspect of the knee is evaluated with the patient in prone position and extended knee. The structures that may be identified are the posterior horns of the menisci, posterior cruciate ligament, the popliteal neurovascular bundle, and the presence of a Baker cyst [20]. The transducer is placed in the transverse plane of the mid-calf to identify the deep soleus and medial and lateral heads of the gastrocnemius muscles. The medial head of the gastrocnemius is followed proximally until the semimembranosus tendon is identified medially. If a Baker cyst is present, it will be visualized between these two structures.

5.3 Patellar tendon

The patellar tendon is part of the extensor mechanism of the knee, which originates at the patellar apex and inserts at the tibial tuberosity. It is located anteriorly to Hoffa's fat pad, and is usually about half of the thickness of the quadriceps

Figure 5.
Quadriceps and patellar tendons showing the dark signal qualities on PDWI.

tendon (approximately 0.5 cm), as seen on sagittal MRI with low homogeneous signal in all sequences (**Figure 5**) [18]. When visualizing it with ultrasound, the patellar tendon should normally exhibit an echogenic, fibrillar appearance. Deep to the tendon, Hoffa's fat pad appears hyperechoic or isoechoic to muscle. The region around the distal patellar tendon is also evaluated for infrapatellar bursal fluid.

Focal patellar tendinosis of the proximal deep insertional fibers is termed jumper's knee in adults, usually presenting as pain in the inferior patellar region. It is often visualized on MRI as thickening of the proximal patellar tendon with increased signal on T2W images [21]. A similar finding in children (often associated with cerebral palsy) is known as Sinding-Larsen-Johansson disease. A complete rupture of the tendon is usually easily identified, due to the secondary finding of a patella alta.

Ultrasound can be very useful in the evaluation of tendinosis and partial tears. Tendinosis will appear as focal or diffuse hypoechogenicity and thickening of the tendon. Partial-thickness tear may reveal similar findings with possible anechoic interstitial clefts. Marked hyperemia from neovascularity may also be identified with color Doppler imaging [22]. Full-thickness tears are seen as complete tendon fiber discontinuity and refraction shadowing at the retracted torn tendon stumps [20].

6. Hip joint

6.1 MRI protocol

MRI evaluation of the hip is performed while the patient is in the supine position. Coronal, axial, sagittal and axial oblique planes are obtained for

MR sequences of the entire pelvis and unilateral symptomatic hip. Imaging sequences of the hip are performed with bilateral legs placed in 15° of internal rotation. Hip MRI generally includes the following imaging sequences: non-fat saturated T1WI, fat saturated T2WI, PD fat saturated images and inversion recovery (IR) images [23].

6.2 Ultrasound examination technique

Examination can be divided in the following approaches [24, 25]:

1. Anterior hip: Patient lies supine with hip in neutral position. Examination starts with the anterior synovial recess, for which the transducer is placed over the femoral head in the oblique longitudinal plane. Examination continues with identifying the anterior glenoid labrum, located cranially in this plane, and the iliofemoral ligament that lies superficially in relation to the labrum. Next, the transducer is placed at the interphase between the femoral head and the joint space to examine the iliopsoas muscle and tendon. The neurovascular bundle and the iliopectineal eminence are used as anatomical landmarks to identify these structures. Lateral to the neurovascular bundle, the iliopsoas muscle is visualized. The iliopsoas tendon lies deep within the bellies of the muscle and on top of the iliopectineal eminence. The adjacent bursa is identified if there is a pathologic process present.

2. Medial hip: Patient remains in the supine position, now with abduction and external rotation of the hip and flexion of the knee. Examination starts in the long axis plane to scan over the insertion of the iliopsoas tendon at the lesser trochanter of the femur. Next, the adductor muscles are evaluated in the axial plane. The muscles of the medial hip compartment are divided in three layers. The adductor longus is located at the lateral aspect of the superficial muscular layer, while the gracilis is located at the medial aspect. The adductor brevis makes up the intermediate muscular layer and the adductor magnus makes up the deep muscular layer. Scan continues in the long axis plane with the transducer moved along the abductor muscles to identify the abductor longus tendon, using the pubic bone as reference landmark. The adductor longus tendon insertion is identified as a hypoechoic triangular structure. Lastly, the transducer is placed over the pubis in the transverse plane, from which oblique longitudinal plane is achieved to evaluate the tendon complex formed by the transversus abdominis and internal oblique muscles.

3. Lateral hip: The patient is moved to the lateral decubitus position, lying on opposite hip of interest. With this examination, the following structures are evaluated: abductor muscles, gluteus medius, gluteus minimus, and tensor fascia lata. To begin, the transducer is placed over the greater trochanter. Scanning is performed in the transverse and longitudinal planes. The gluteus medius, seen as a curvilinear fibrillar band, lies superficial to the gluteus minimus. The tensor fascia lata serves as an anatomical landmark to identify the gluteus muscles, which is visualized as a superficial hyperechoic band in the coronal plane.

4. Posterior hip: Evaluated with the patient in the prone position. Important structures to evaluate include: the hamstring muscles and the sciatic nerve. Examination starts in the transverse plane with the transducer positioned at the ischial tuberosity to identify the hamstring tendon complex, where no distinction can be made between each individual tendon. The sciatic nerve is a lateral flattened structure with fascicular echotexture. As the transducer is

moved caudally, distinction between individual hamstring tendons is achieved with the semimembranosus tendon located deep and medially in relation to the conjoined tendon complex of the biceps femoris and semimembranosus. Sonographic appearance of this conjoined tendon complex is a hyperechoic line that separates the laterally located biceps femoris muscular belly from the medially located semimembranosus muscular belly.

6.3 Gluteal tendons

The gluteus medius and gluteus minimus tendons are part of the lateral compartment of the hip. The gluteus medius tendon inserts at the lateral and superoposterior facets of the greater trochanter of the femur, while the gluteus minimus tendon inserts at the anterior aspect of the greater trochanter. Ultrasound shows the gluteus medius tendon as a hyperechoic structure arising from a fan shaped hypoechoic structure that represents the gluteus medius muscle. The gluteus medius and minimus muscles are separated by an echogenic layer of fascia and adipose tissue [26].

The gluteus medius and minimus are the most commonly affected tendons of the hip abductor group that cause greater trochanteric pain syndrome [28]. Gluteus tendon abnormalities may be due to acute injury or chronic wear and tear of the hip joint. Therefore, it typically affects women in the middle and elderly age groups.

MRI is the gold standard imaging modality for the identification of gluteus tendon tears (**Figure 6**). Axial and coronal T2W fat saturated images of the hip and coronal T1WI of the pelvis are recommended when abductor tendon pathology is suspected [29]. MRI diagnostic criteria for tendon tears include discontinuity of the tendon, elongation of the gluteus medius 2 cm or greater and T2 hyperintensities superior to the level of the greater trochanter of the femur [27]. Additional MR findings, although nonspecific, may include atrophy of the adipose tissue, changes of the adjacent bone structures and fluid collection within the bursa.

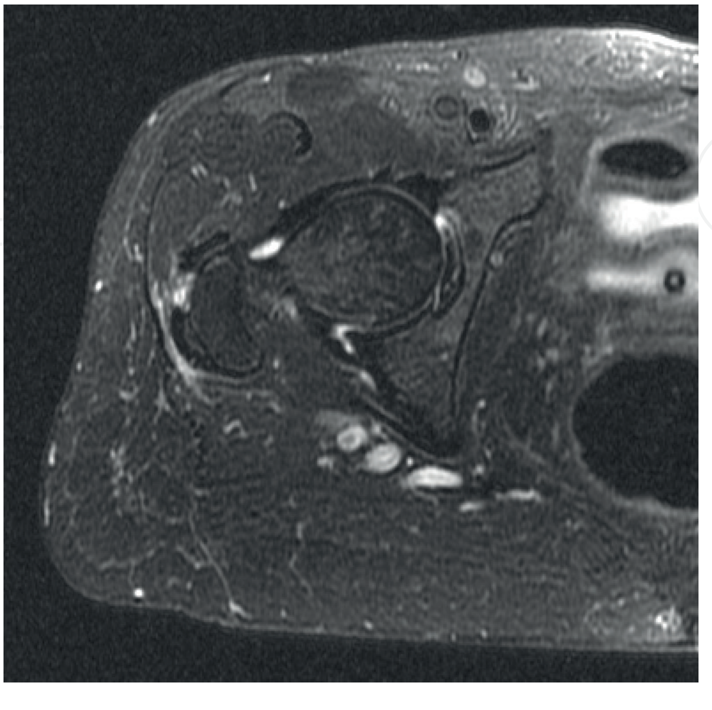

Figure 6.
T2 fat saturated axial image shows a full thickness tear of the gluteus medius tendon as a fluid-filled defect along the greater trochanter.

6.4 Iliopsoas tendon

The psoas major and iliacus muscles form the iliopsoas tendon complex. The psoas major originates at the transverse processes of L1-L5 vertebrae; while the iliacus muscle has various origins, including the superior two thirds of the iliac fossa, the anterior sacroiliac ligaments, and the anterior sacral ala. This tendon complex inserts at the lesser trochanter of the femur.

The iliopsoas tendon has an echogenic sonographic imaging appearance, with anterior extension in relation to the anterior-superior acetabular labrum [28]. On MRI sequences, the iliopsoas tendon complex is characteristically identified as two parallel homogeneously hypointense structures, separated by a hyperintense region that represents adipose tissue of the fascia [28].

Snapping iliopsoas tendon is characterized by an audible or palpable painful snap with movement of the hip. Repetitive movements of the hip serve as predisposition to develop a snapping tendon, such as those performed by young athletes in different sports, with ballet dancers being the most commonly affected [30]. Iliopsoas tendon as the source of a snapping hip is classified as an internal cause of the broader term snapping hip syndrome. It may get trapped during movement due to a prominent iliopectineal eminence, an insertion site osseous projection or the anterior inferior aspect of the iliac spine [30].

Dynamic evaluation of the hip joint with US and MRI allows the identification of the source of snapping iliopsoas tendon. Sonographic evaluation is performed with a high-frequency transducer (linear 5–12 MHz) placed in the transverse oblique plane, above the hip joint and parallel to the pubis [28]. The patient is in the supine position, with initial static evaluation performed following the iliopsoas tendon until reaching its insertion at the lesser trochanter. Dynamic evaluation is performed while the ipsilateral leg is moved from the "frog leg" position (extension, adduction, and internal rotation) to the neutral position (flexion, abduction, and external rotation). The position of the iliopsoas tendon can be traced along the anterior compartment of the hip as the leg is moved from the aforementioned positions and snapping occurs. Regarding MRI examination for this particular pathology, fast GRE sequence allows dynamic evaluation of the iliopsoas tendon during movement [28]; change from "frog leg" to neutral position is also performed during this MRI sequence.

6.5 Hamstring tendons

The hamstring tendon complex is located at the posterior compartment of the hip, formed by three muscles groups: biceps femoris, semimembranosus and semitendinosus. The biceps femoris is composed of a short and a long head. Origin of the short head is at the lateral linea aspera of the posterior femur, the lateral supracondylar line and the intermuscular septum [31]. The long head shares origin with the semitendinosus tendon at the inferomedial facet of the ischial tuberosity to form a conjoint tendon. Distal biceps femoris tendon inserts at the lateral fibular head and lateral condyle of proximal tibia, while the semitendinosus inserts at the anteromedial aspect of the tibia, sharing insertion with the gracilis and sartorius muscles to form the pes anserinus tendons [32]. The semimembranosus tendon originates at the superolateral ischial tuberosity and has several insertion sites through tendinous arms [31]. The anterior, direct, and inferior arms insert at the medial condyle of the tibia. The capsular arm inserts at the posterior oblique ligament. There is also insertion into the posterior joint capsule and arcuate ligament through the oblique popliteal ligament.

On MRI sequences at the level of the ischial tuberosity, the hamstring tendons are identified as well-defined round areas of low signal intensity, where the conjoint tendon is posteromedial to the semimembranosus tendon [31].

The hamstrings are the most commonly injured muscle group in athletes, with tendon avulsion as the most severe injury diagnosed with medical imaging, requiring prompt surgical management. Avulsion injuries are defined as complete tear of the tendon from its osseous insertion site and typically affect the hamstrings proximally, particularly the conjoint tendon. This type of injury can include pulling of a bone piece by the torn tendon, which most commonly occurs in children due to presence of growth plates. MRI is the gold standard for examination of suspected hamstring tendon avulsion. Evaluation approach involves identifying the affected tendon and determining whether a partial or full thickness tear occurred. In the case of full thickness tears, distal tendon retraction, degree of underlying tendinopathy, and proximity of the tear to the sciatic nerve must be included in the evaluation approach [32].

7. Ankle

7.1 MRI protocol

The ankle tendons are visualized as low signal intensity structures in all MR sequences. The T1WI sequences are used to evaluate the anatomy and the T2W sequences are used to assess abnormal increase in fluid, usually related to tendon pathology [33]. Axial images are used to evaluate morphologic features of the tendons and synovial sheath distention, longitudinal splits, fluid within the tendon sheath, and adjacent soft tissue abnormalities, if any. For evaluating the Achilles tendon, sagittal images prove most useful. Sagittal images also assess the proximal-to-distal extent of tendon pathologies. Oblique coronal or short axis images at the level of the mid- and forefoot are best for assessment of the tendons distal to the ankle [33, 34].

When the normal tendons form an angle of approximately 55° with the main magnetic vector, it produces increased signal intensity within the tendons. This phenomenon is called the magic angle, more commonly in sequences with echo times less than 20 msec (T1WI, PD or GRE). This effect is particularly common with ankle tendons because of their curvatures around the ankle joint [33, 34].

For general purposes, an ankle MRI should include at least the following: axial T1WI or PD sequences and fat-suppressed T2WI, coronal T1WI or fat-suppressed T2WI and IR sagittal images [34].

7.2 Ultrasound examination technique

1. Peroneal tendon: Evaluated with the patient in the supine position with the knee semi-flexed and the ankle in internal rotation. For evaluation of the plantar aspect of the peroneus longus tendon, the patient should be in the prone position [35]. Both peroneal tendons are examined with linear transducers in their short and long planes. The transducer is placed behind the lateral malleolus over the tendons to examine their short-axis first. The transducer should be tilted along the way, to maintain the perpendicular position of the US beam. The tendons should be evaluated upwards for approximately 5 cm and downwards into the inframalleolar region [34, 36, 37].

2. Posterior tibial tendon: Evaluated with the patient in a seated position with internal rotation of the plantar surface of the foot. If this position cannot be

achieved, the patient may lie supine with the foot slightly laterally rotated. Placing the transducer in short-axis/transverse position behind the medial malleolus, evaluate the posterior tibial tendon following it from its myotendinous junction into its insertion [36].

3. Achilles tendon: Evaluated with the patient in prone position and the foot hanging from the examination table. With the transducer, follow the tendon from its myotendinous junction downward to its calcaneal insertion in both the short and long planes. The size of the tendon should only be obtained in the transverse plane [36].

7.3 Peroneal tendon

The peroneal tendons are the third most commonly injured tendons of the ankle. Acute and chronic tears occur in young, athletic patients due to overuse or in older patients with multifactorial degenerative wear and tear. Due to their course and location, calcaneal fractures predispose to partial tears, entrapment and dislocation of the peroneal tendons. Tendinopathy more commonly affects the peroneus brevis tendon. Split peroneus brevis syndrome represents a longitudinal tear of the tendon and the term arises from the fact that the peroneus brevis tendon is usually located anteriorly, is embedded between the peroneus longus and fibula [33, 34, 38].

7.4 Tibialis posterior tendon

The tibialis posterior tendon is the second most commonly injured of the ankle tendons [37]. It should never have more than twice the cross-sectional area of the flexor digitorum longus tendon. Posterior tibial tendinopathy occurs because of delayed stretching of the tendon due to chronic micro-tears, and usually occurs in older women with progressively painful flat-foot. Systemic diseases like rheumatoid arthritis and diabetes predispose this condition, as for other tendinopathies. On MR and ultrasound imaging it will appear as tendon thickening with loss of normal echogenicity and tendon sheath fluid, with increased T2 signal intensity. Imaging pitfalls include: normal tendon widening at its insertion onto the navicular bone; fluid within the tendon sheath, mimicking enlargement on T1W sequences; and magic angle phenomenon [33, 37, 39]. Due to its course and insertion, abnormalities of the navicular bone may predispose to tibialis posterior tendinopathy; like the type II accessory navicular bone or *os naviculare,* which is typically large and closely positioned at the medial pole of the navicular bone by a synchondrosis, rendering insertion of the posterior tibial tendon only on this ossicle and not extending into the cuneiforms and metatarsals [36].

7.5 Achilles tendon

The Achilles tendon is the most commonly injured tendon of the ankle (**Figure 7**) [37]. It is usually hypointense on all MR sequences, although due to its fascicular anatomy, a single line may be visible (not on T2WI), mimicking an interstitial tear. Punctate foci of increased signal intensity may be noted in axial images of the distal Achilles tendon, which simply are interfascicular membranes. Normal average thickness is 6–8 mm, which may increase in male, tall and elderly patients. On axial images its margins are concave for the majority of its course, being more convex proximally to and at the soleus insertion. Normally, there should be subcutaneous fat between the Achilles tendon and the skin. Branches of the posterior tibial artery supply the Achilles tendon, but blood supply diminishes at approximately 2–6 cm proximal to its insertion site, making this region of decreased vascularity particularly susceptible to ruptures [35, 37].

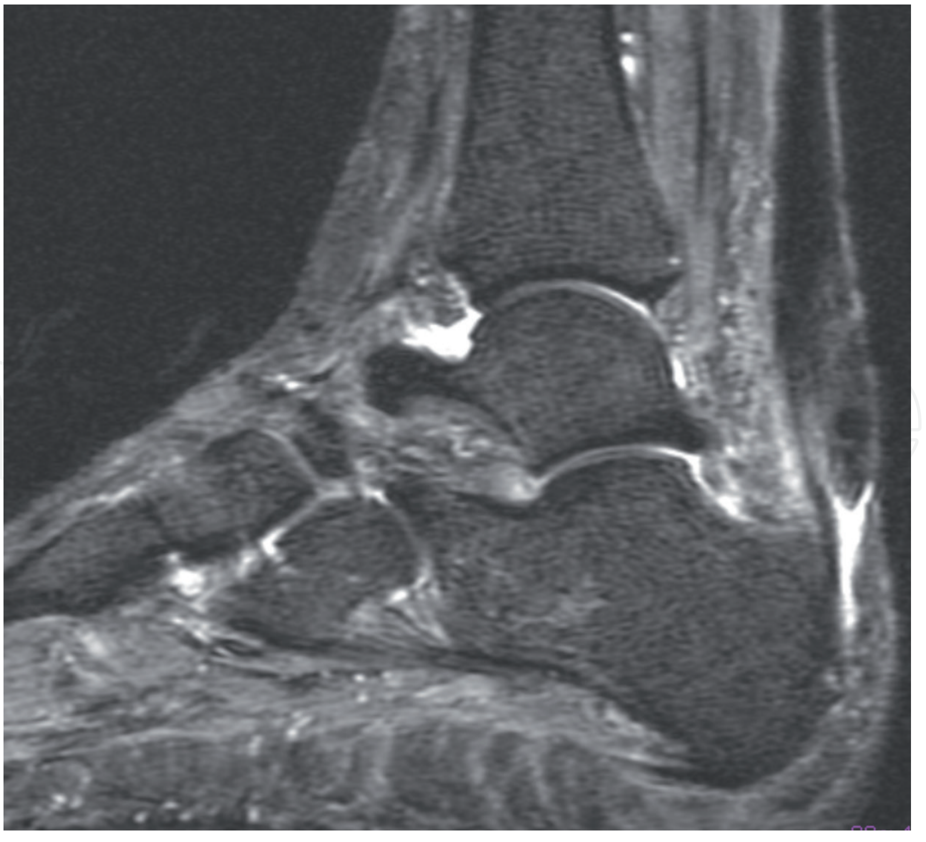

Figure 7.
T2 fat saturated sagittal image shows disruption of the distal Achilles tendon with a fluid-filled gap.

Achilles tendinosis is common in runners and jumpers. In Achilles tendinosis and peritendinosis, the tendon may enlarge. Acute Achilles ruptures more commonly occur in patients with chronic tendinopathy; runners, middle-aged women who engage in sporadic exercise or patients with systemic diseases or chronic steroid use, resulting in a weakened tendon. Most common site of Achilles tendon rupture is 2–6 cm proximal to its insertion site, avascular zone, as detailed above. Acute ruptures show a tendon gap with intermediate signal intensity on T1WI and increased signal intensity on T2WI, consistent with edema and hemorrhage. In chronic ruptures the gap is replaced by fat and scar tissue [33, 35, 37]. An accessory soleus muscle may be mistaken with a thickened Achilles tendon, which differ by their signal intensity on MRI. Achilles tendon thickening may occur after surgical procedures. There is thickening also with of xanthomas (familial hyperlipidemia) that appear as marked tendon enlargement with heterogeneous signal masses and linear areas of low signal intensity. Haglund's disease results most commonly from ill-fitting shoes that compress the distal Achilles tendon, leading to peritendinous edema, retrocalcaneal bursitis and tendon thickening [37].

8. Conclusion

MRI and US are useful imaging modalities that allow anatomic evaluation of tendons as well as identification of tendon pathology.

Acknowledgements

Thanks to the University of Puerto Rico School of Medicine Diagnostic Radiology Department for allowing us to use images from its teaching file.

Conflict of interest

None.

Acronyms and abbreviations

MRI	magnetic resonance imaging
US	ultrasound
T1WI	T1-weighted image
FSE	fast spin echo
T2WI	T2-weighted image
PD	proton density
GRE	gradient echo
APL	abductor pollicis longus
EPB	extensor pollicis brevis
LCL	lateral collateral ligament
IR	inversion recovery

Author details

Stephanie C. Torres-Ayala[1*], Alvaro Bravo-Martínez[1], Amanda P. Marrero-González[1], Luis R. Rodriguez-Ortíz[1] and Jorge A. Vidal[2,3]

1 University of Puerto Rico School of Medicine Diagnostic Radiology, San Juan, Puerto Rico, USA

2 University of Puerto Rico School of Medicine, Musculoskeletal Radiology Section, San Juan, Puerto Rico, USA

3 University of Alabama at Birmingham, Emergency Radiology Section, Birmingham, Alabama, USA

*Address all correspondence to: stephanie.torres19@upr.edu

References

[1] Chen Q, Miller TT, Padron M, Beltran J. Normal shoulder. In: Musculoskeletal Imaging. 2nd ed. Philadelphia, PA: Elsevier; 2015. pp. 70-86

[2] Singh JP. Shoulder ultrasound: What you need to know. Indian Journal of Radiology and Imaging. 2012;**22**(4):284-292. DOI: 10.4103/0971-3026.111481

[3] Jacobson JA. Shoulder US: Anatomy, technique, and scanning pitfalls. Radiology. 2011;**260**(1):6-16. DOI: 10.1148/radiol.11101082

[4] Crass JR, Craig EV, Feinberg SB. The hyperextended internal rotation view in rotator cuff ultrasonography. Journal of Clinical Ultrasound. 1987;**15**(6):416-420

[5] Ferry M, Finlay K, Popowich T, Stamp G, Schuringa P, Friedman L. Sonography of full-thickness supraspinatus tears: Comparison of patient positioning technique with surgical correlation. American Journal of Roentgenology. 2005;**184**(1):180-184. DOI: 10.2298/SARH0912647S

[6] Arend CF, Silva TR. Comparison between exclusively long-axis and multiple-axis sonographic protocols for screening of rotator cuff lesions in symptomatic shoulders. Journal of Ultrasound in Medicine. 2010;**29**:1725-1732

[7] Helms CA, Major NM, Anderson MW, Kaplan PA, Dussault R. Shoulder. In: Musculoskeletal MRI. 2nd ed. Philadelphia, PA: Elsevier; 2009. pp. 177-223

[8] Jacobson JA. Shoulder ultrasound. In: Fundamentals of Musculoskeletal Ultrasound. 3rd ed. Philadelphia, PA: Elsevier; 2018. pp. 55-126

[9] Skendzel JG, Jacobson JA, Carpenter JE, et al. Long head of biceps brachii tendon evaluation: Accuracy of preoperative ultrasound. AJR. American Journal of Roentgenology. 2011;**197**:942-948. DOI: 10.2214/AJR.10.5012

[10] Sampath SC, Sampath SC, Bredella MA, et al. Magnetic resonance imaging of the elbow. Sports Health. 2013;**5**(1):34-39. DOI: 10.1177/1941738112467941

[11] Konin GP, Nazarian LN, Walz DM. US of the elbow: Indications, technique, normal anatomy, and pathologic conditions. Radiographics. 2013;**33**(4):125-127. DOI: 10.1148/rg.334125059

[12] Bucknor MD, Stevens KJ, Steinbach LS. Elbow imaging in sports: Sports imaging series. Radiology. 2016;**279**(3):827-837. DOI: 10.1148/radiol.2016151256

[13] Kassarjian A, Benjamin L, Afonso D, et al. Guidelines for MR Imaging Sports Injuries. European Society of Skeletal Radiology Sub-committee [Internet]. 2016. Available from: https://essr.org/content-essr/uploads/2016/10/ESSR-MRI-Protocols-Thumb.pdf

[14] Gupta P, Lenchik L, Wuertzer SD, et al. High-resolution 3-T MRI of the fingers: Review of anatomy and common tendon and ligament injuries. American Journal of Roentgenology. 2015;**204**(3):W314-W323. DOI: 10.2214/AJR.14.12776

[15] Glajchen N, Schweitzer M. MRI features in de Quervain's tenosynovitis of the wrist. Skeletal Radiology. 1996;**25**(1):63-65. DOI: 10.1007/s002560050033

[16] Guerini H, Pessi E, Theumann N, et al. Sonographic appearance of trigger fingers. Journal of Ultrasound in Medicine. 2008;**27**(10):1407-1413. DOI: 0278-4297/08/$3.50

[17] Helms CA, Major NM, Anderson MW, Kaplan PA, Dussault R. Knee. In: Musculoskeletal MRI. 2nd ed. Philadelphia, PA: Elsevier; 2009. pp. 353-383

[18] De Maeseneer MO, Shahabpour M. Normal knee. In: Musculoskeletal Imaging. 2nd ed. Philadelphia, PA: Elsevier; 2015. pp. 324-332

[19] Alves TI, Girish G, Kalume brigido M, Jacobson JA. US of the knee: Scanning techniques, pitfalls, and pathologic conditions. Radiographics. 2016;**36**(6):1759-1775. DOI: 10.1148/rg.2016160019

[20] Jacobson JA. Knee ultrasound. In: Fundamentals of Musculoskeletal Ultrasound. 3rd ed. Philadelphia, PA: Elsevier; 2018. pp. 284-327

[21] Yus JS, Popp JE, Kaeding CC, Lucas J. Correlation of MR imaging and pathologic findings in athletes undergoing surgery for chronic patellar tendinitis. American Journal of Roentgenology. 1995;**165**:115-118. DOI: 10.2214/ajr.165.1.7785569

[22] Khan KM, Bonar F, Desomnd PM, et al. Patellar tendinosis (jumper's knee): Findings at histopathologic examination, US, and MR imaging-Victorian Institute of Sport Tendon Study Group. Radiology. 1996;**200**(3):821-827. DOI: 10.1148/radiology.200.3.8.8756939

[23] Kassarjian A, Fritz B, Afonso PD, Alcalá-Galiano A, Ereño MJ, Grainger A, et al. Guidelines for MR Imaging of the Hip Region [Internet]. 2016. Available from: essr.org/content-essr/uploads/2016/10/ESSR_Sports_guidelines.pdf [Accessed: November 19, 2018]

[24] Beggs I, Bianchi S, Bueno A, Cohen M, Court-Payen M, Grainger A, et al. Musculoskeletal Ultrasound Technical Guidelines IV. Hip [Internet]. 2016. Available from: https://essr.org/content-essr/uploads/2016/10/hip.pdf [Accessed: November 19, 2018]

[25] Lin YT, Wang TG. Ultrasonographic examination of the adult hip. Journal of Medical Ultrasound. 2012;**20**(4):201-209. DOI: 10.1016/j.jmu.2012.10.009

[26] Connell DA, Bass C, Sykes CA, Young D, Edwards E. Sonographic evaluation of gluteus medius and minimus tendinopathy. European Radiology. 2003;**13**(6):1339-1347. DOI: 10.1007/s00330-002-1740-4

[27] Cvitanic O, Henzie G, Skezas N, Lyons J, Minter J. MRI diagnosis of tears of the hip abductor tendons (gluteus medius and gluteus minimus). American Journal of Roentgenology. 2004;**182**(1):137-143. DOI: 10.2214/ajr.182.1.1820137

[28] Bancroft LW, Blankenbaker DG. Imaging of the tendons about the pelvis. American Journal of Roentgenology. 2010;**195**(3):605-617. DOI: 10.2214/ajr.10.4682

[29] Hartigan DE, Perets I, Walsh JP, Domb BG. Imaging of abductor tears: Stepwise technique for accurate diagnosis. Arthroscopy Techniques. 2017;**6**(5):e1523-e1527. DOI: 10.1016/j.eats.2017.06.032

[30] Piechota M, Maczuch J, Skupinski J, Kulawska-Sysio K, Wawrzynek W. Internal snapping hip syndrome in dynamic ultrasonography. Journal of Ultrasonography. 2016;**16**(66):296-303. DOI: 10.15557/JoU.2016.0030

[31] Koulouris G, Connell D. Hamstring muscle complex: An imaging review. Radiographics. 2005;**25**(3):571-586. DOI: 10.1148/rg.253045711

[32] Rubin DA. Imaging diagnosis and prognostication of hamstring injuries. American Journal of Roentgenology. 2012;**199**(3):525-533. DOI: 10.2214/ajr.12.8784

[33] Rosenberg ZS, Beltran J, Bencardino JT. From the RSNA refresher courses MR imaging of the ankle and foot. Radiographics. 2000;**20**:153-179. DOI: 10.1148/radiographics.20.suppl_1.g00oc26s153

[34] Wang X-T, Rosenberg ZS, Mechlin MB, Schweitzer ME. Normal variants and diseases of the peroneal tendons and superior peroneal retinaculum: MR imaging features. Radiographics. 2005;**25**:587-602. DOI: 10.1148/rg.253045123

[35] Schweitzer ME, Karasick D. MR imaging of disorders of the Achilles tendon. American Journal of Roentgenology. 2000;**175**:613-625

[36] Beggs I, Bianchi S, Bueno A, Cohen M, Court-Payen M, Grainger A, et al. Musculoskeletal ultrasound: technical guidelines. Insights into Imaging. 2010;**1**:99-141. DOI: 10.1007/s13244-010-0032-9

[37] Manaster BJ, May DA, Disler DG. Musculoskeletal Imaging: The Requisites. 4th ed. Saunders: Elsevier; 2013. pp. 215-234. DOI: 978-0-323-08177-1.ch14

[38] Taljanovic MS, Alcala JN, Gimber LH, Rieke JD, Chilvers MM, Latt LD. High-resolution US and MR imaging of peroneal tendon injuries. Radiographics. 2015;**35**:179-199. DOI: 10.1148/rg.351130062

[39] Schweitzer ME, Karasick D. MR imaging of disorders of the posterior tibialis tendon. American Journal of Roentgenology. 2000;**175**:627-635. DOI: 10.2214/ajr.175.3.1750627